British Journal of Pharmacology (2006) 149, 931–941

0007–1188/06 $30.00
www.brjpharmacol.org

RESEARCH PAPER

Mechanisms underlying lysophosphatidylcholine-induced potentiation of vascular contractions in the Otsuka Long-Evans Tokushima Fatty (OLETF) rat aorta

T Matsumoto, T Kobayashi and K Kamata

Department of Physiology and Morphology, Institute of Medicinal Chemistry, Hoshi University, Shinagawa-ku, Tokyo, Japan

Background and purpose: The effect of lysophosphatidylcholine (LPC) on aortic contractions in Otsuka Long-Evans Tokushima Fatty (OLETF) rats, a type 2 diabetic model, was studied.
Experimental approach: Using OLETF rats and control (Long Evans Tokushima Otsuka (LETO)) rats, the effects of LPC on the contractions induced by high-K^+ (10-40 mM), UK14,304 (10∼100 nM; a selective α_2-adrenoceptor agonist) and sodium orthovanadate (SOV; 10 μM∼3 mM) in endothelium-denuded aortae were compared. Aortic ERK activity and the mRNA expression for GPR4 (a putative LPC receptor) were also measured.
Key results: OLETF rats exhibited (vs. age-matched LETO rats): (1) greater potentiation of high-K^+-induced contraction by 10 μM LPC – a potentiation attenuated by 10 μM genistein, protein tyrosine kinase (PTK) inhibitor, (2) greater potentiation of UK14,304 (10∼100 nM)-induced contractions by LPC (1 μM∼10 μM) – a potentiation attenuated by 10 μM genistein, 50 μM tyrphostin A23 (PTK inhibitor) or 10 μM PD98059 (MEK 1/2 inhibitor), (3) greater basal and LPC (1 μM)-induced ERK activities, (4) greater basal and 100 nM UK14,304-stimulated ERK2 activities in both the absence and presence of 10 μM LPC, (5) greater SOV (10 μM∼3 mM)-induced contractions, (6) greater potentiation of SOV-induced contractions by 10 μM LPC – a potentiation suppressed by 10 μM PD98059 or 10 μM genistein, (7) upregulation of GPR4 mRNA.
Conclusions and implications: These results suggest that the LPC-induced potentiation of contractions in the OLETF rat aorta may be attributable to increased PTKs or ERK activity and/or to receptor upregulation.
British Journal of Pharmacology (2006) **149,** 931–941. doi:10.1038/sj.bjp.0706937; published online 9 October 2006

Keywords: aorta; contraction; LPC; tyrosine kinase; type II diabetes; ERK

Abbreviations: AEBSF, 4-(2-aminoethyl)benzenesulphonyl fluoride hydrochloride; EDTA, ethylenediaminetetraacetic acid; ELISA, enzyme-linked immunosorbent assay; ERK, extracellular signal-regulated kinase; G2A, G2 accumulation; GAPDH, glyceraldehydes-3-phosphate dihydrogenase; GPR4, G-protein-coupled receptor 4; KHS, Krebs–Henseleit solution; LDL, low-density lipoprotein; LETO, Long–Evans Tokushima Otsuka; LPC, lysophosphatidylcholine; MDA, malondialdehyde; MEK, mitogen-activated protein kinase kinase; OLETF, Otsuka Long–Evans Tokushima Fatty; PD98059, 2′-amino-3′-methoxyflavone; PTK, protein tyrosine kinase; RT–PCR, reverse transcription-polymerase chain reaction; SOD, superoxide dismutase; SOV, sodium orthovanadate; TNF-α, tumour necrosis factor-α; UK14, 304, 5′-bromo-6-[2-imidazolin-2-yl-amino]-quinoxaline; vWF, von Willebrand factor

Introduction

Diabetes mellitus is a strong risk factor for all manifestations of atherosclerotic vascular disease (De Vriese *et al*., 2000; Luscher *et al*., 2003). Although the pathophysiological mechanisms underlying the development of atherosclerosis in diabetic patients have not been fully elucidated, it is thought that hyperlipidaemia, increased oxidation of low-density lipoprotein (LDL) and impaired vascular function promote atherogenesis in such patients. In addition, several epidemiological studies on diabetic and non-diabetic patients have shown an association between the insulin resistance and/or hyperinsulinaemia associated with type II

Correspondence: Professor K Kamata, Department of Physiology and Morphology, Institute of Medicinal Chemistry, Hoshi University, Shinagawa-ku, Tokyo 142-8501, Japan.
E-mail: kamata@hoshi.ac.jp
Received 3 May 2006; revised 4 September 2006; accepted 7 September 2006; published online 9 October 2006

diabetes and atherosclerotic disorders such as cardiovascular disease (Luscher *et al*., 2003), which is one of the major causes of death in diabetic patients.

Lysophosphatidylcholine (LPC) belongs to a group of bioactive glycerol- or sphingosine-based lysophospholipids (i.e. lysophosphatidic acid, sphingosine-1-phosphate and sphingosylphosphorylcholine) generated from membrane phospholipids as part of normal physiological activities or disease processes (McIntyre *et al*., 1999). LPC is also a major phospholipid component (40–50%) of oxidized LDL (McIntyre *et al*., 1999) and is implicated as a critical atherogenic factor of oxidized LDL. Interestingly, plasma LPC concentrations are increased in both type I and type II diabetic patients compared with control subjects (Rabini *et al*., 1994). Despite these documented elevations of LPC in association with pathological conditions, the pathophysiological role of LPC in diabetic states remains to be established.

LPC can activate several second messenger pathways, including protein kinase C, extracellular signal-regulated kinases (ERKs), protein tyrosine kinases (PTKs) and Ca^{2+} (Chen *et al*., 1995; Ozaki *et al*., 1999), implicating the engagement of transduction mechanisms. Further, current evidence suggests that LPC inhibits endothelium-dependent relaxations mediated by endothelium-derived relaxing factor, and it is likely that LPC causes vascular spasm (Kugiyama *et al*., 1990; Kamata and Nakajima, 1998; Matsumoto *et al*., 2006b). In addition, we found in the rat endothelium-denuded aorta that while LPC did not itself produce contraction, it did potentiate the vascular contractile responses induced by high-K^+, UK14,304 (5′-bromo-6-[2-imidazolin-2-yl-amino]-quinoxaline) (a selective α_2-adrenoceptor agonist) and phorbol ester (Suenaga and Kamata, 1998). Moreover, we recently showed that the potentiating effect of LPC is accompanied by an increase in the tyrosine phosphorylation of proteins and that both genistein and tyrophostin B42 attenuated the potentiating effect of LPC on high-K^+-induced contraction (Suenaga and Kamata, 2002). We later found that this potentiating effect of LPC in the rat aorta involved ERK activation and a consequent regulation of Ca^{2+} influx (Suenaga and Kamata, 2003). Moreover, recent evidence suggests that two cloned orphan G-protein-coupled receptors, G-protein-coupled receptor 4 (GPR4) and G2A, may serve as specific LPC receptors in several cells (Zhu *et al*., 2001; Xu, 2002), the ectopically expressed receptors demonstrating high affinity and specificity for LPC. Also, Rikitake *et al*. (2002) demonstrated that G2A was abundantly expressed in monocytes/macrophages, but not in vascular endothelial and smooth muscle cells. Whereas, Lum *et al*. (2003) found that while GPR4 mRNA was expressed in human vascular endothelial cells, G2A was not, and they suggested that in endothelial cells, endogenous GPR4 may be a potential G-protein-coupled receptor by which LPC signals proinflammatory activities. However, the physiological function and endogenous expression of LPC receptors in vascular smooth muscle as well as the pathological implications for type II diabetes have yet to be fully elucidated.

The aim of the present study was to investigate whether the enhancing effect of LPC on contractile responses in the aorta might be altered in type II diabetic rats (Otsuka Long–Evans Tokushima Fatty (OLETF) rats). We also determined whether aortae from Long–Evans Tokushima Otsuka (LETO) rats, a genetic control for OLETF, differ from OLETF rat aortae in their GPR4 expression profile.

Methods

Animals and experimental design

Five-week-old male rats (OLETF rats and LETO rats, a genetic control for OLETF) were supplied by the Tokushima Research Institute (Otsuka Pharmaceutical). Food and water were given *ad libitum* in a controlled environment (room temperature 21–22°C, room humidity 50 ± 5%) until the rats were 60 weeks old. This study was approved by the Hoshi University Animal Care and Use Committee, and all studies were conducted in accordance with 'Guide for the Care and Use of Laboratory Animals' published by the US National Institute of Health, and 'Guide for the Care and Use of Laboratory Animals' adopted by the Committee on the Care and Use of Laboratory Animals of Hoshi University (which is accredited by the Ministry of Education, Culture, Sports, Science and Technology, Japan).

Measurement of plasma glucose, cholesterol, triglyceride, insulin, malondialdehyde, superoxide dismutase activity and blood pressure

Plasma parameters and blood pressure were measured as described previously (Matsumoto *et al*., 2003, 2004a, 2005, 2006b; Kobayashi *et al*., 2004). Briefly, plasma glucose, cholesterol and triglyceride levels, and superoxide dismutase (SOD) activity were each determined by the use of a commercially available enzyme kit (Wako Chemical Company, Osaka, Japan). High-density lipoprotein (HDL) cholesterol was measured following phosphotungstic-$MgCl_2$ precipitation of apolipoprotein B containing very-low-density lipoprotein. The LDL level was derived from the above data using the Friedewald formula: LDL cholesterol = total cholesterol − HDL − (1/5) triglyceride (Friedewald *et al*., 1972). Plasma insulin was measured by enzyme immunoassay (Shibayagi, Gunma, Japan). After a given rat had been in a constant-temperature box at 37°C for a few minutes, its blood pressure was measured by the tail-cuff method using a blood pressure analyser (BP-98A; Softron, Tokyo, Japan). The level of lipid peroxidation product (malondialdehyde (MDA)) was measured using an LPO-586 kit (OxisResearch; Portland, OR, USA). Plasma samples were allowed to react with a chromogenic reagent at 45°C for 60 min. The samples were centrifuged at 15 000 *g* for 10 min at 4°C, and supernatants were measured at 586 nm. The level of MDA was calculated using the standard curve according to the manufacturer's instructions.

Measurement of isometric force

Vascular isometric force was recorded as in our previous papers (Kobayashi *et al*., 2000, 2003; Suenaga and Kamata, 2002, 2003; Matsumoto *et al*., 2004b). Rats were anaesthetized with diethyl ether and killed by decapitation at 60 weeks of age. The thoracic aorta was rapidly dissected out

and placed in ice-cold, oxygenated, modified Krebs–Henseleit solution (KHS). This solution consisted of (in mM) 118.0 NaCl, 4.7 KCl, 25.0 $NaHCO_3$, 1.8 $CaCl_2$, 1.2 NaH_2PO_4, 1.2 $MgSO_4$ and 11.0 dextrose. It was then cleaned of loosely adhering fat and connective tissue and cut into helical strips 2 mm in width and 20 mm in length. The endothelium was removed by rubbing the intimal surface with a cotton swab, successful removal being functionally confirmed by the absence of a relaxation to 10 μM acetylcholine chloride (ACh).

Each aortic strip was suspended in an organ bath containing 10 ml of well-oxygenated (95% O_2 + 5% CO_2) KHS at 37°C. Force generation was monitored by means of an isometric transducer (model TB-611T; Nihon Kohden, Tokyo, Japan). The resting tension in the aortic strip was adjusted to 1.0 g, which was found to be the optimal tension for inducing a maximal contraction in preliminary experiments. The aortic strips were first contracted by 80 mM K^+, these responses being taken as 100%. The mean contractile responses induced by 80 mM K^+ in OLETF ($n=80$) and LETO ($n=79$) were 125.9 ± 3.3 and 135.2 ± 4.0 mg tissue^{-1}, respectively (no significant difference). After washing and equilibrating for 1 h, the aortic strips were treated with a PTK inhibitor (10 μM genistein or 50 μM tyrphostin A23), or with 10 μM daidzein (an inactive isomer of genistein) or a selective mitogen-activated protein kinase kinase (MEK) inhibitor (10 μM 2′-amino-3′-methoxyflavone (PD98059)) for 20 min, then incubated with LPC for 15 min. After this incubation period, high-K^+ or UK14,304 was cumulatively or singly applied.

In separate experiments, to investigate the effect of a tyrosine phosphatase inhibitor on vascular tone, sodium orthovanadate (SOV) (10 μM–3 mM) was cumulatively applied to the aorta. In some of these experiments, 10 μM genistein or 10 μM daidzein was applied 30 min before the SOV application and was present thereafter. In some other experiments, aortic strips were treated with 10 μM genistein, 10 μM daidzein, 10 μM PD98059 or vehicle for 20 min, then incubated with 10 μM LPC for 15 min. After this incubation period, SOV was cumulatively applied. Contractile responses were each expressed as a percentage of the contraction previously induced by 80 mM KCl.

Western blotting

The protein level was quantified using immunoblotting procedures, essentially as described previously (Suenaga and Kamata, 2003). Endothelium-denuded aortic tissues were incubated with LPC (1 or 10 μM) for 15 min. For experiments with inhibitor, tissues were pretreated with 10 μM genistein for 20 min before the addition of 10 μM LPC. Aortic tissues were homogenized in ice-cold lysis buffer containing 250 mM sucrose, 10 mM Tris-HCl (pH 7.5), 5 mM ethylenediaminetetraacetic acid (EDTA), 1 mM 4-(2-aminoethyl)benzenesulphonyl fluoride hydrochloride (AEBSF), 10 μg ml^{-1} aprotinin, 10 μg ml^{-1} leupeptin, 1 mM SOV, 10 mM NaF and 0.1% Triton X-100. The lysate was cleared by centrifugation at 14 000 *g* for 20 min at 4°C. The supernatant was collected and the proteins dissolved in Laemmli's buffer containing mercaptoethanol. The protein concentration was determined by means of a bicinchoninic acid (BCA) protein assay reagent kit (Pierce, Rockford, IL, USA). Samples (10 μg lane^{-1}) were resolved by electrophoresis on 7.5% sodium dodecyl sulphate–polyacrylamide gel electrophoresis gels, then transferred onto polyvinylidene fluoride membranes. Briefly, after blocking the residual protein sites on the membrane with Block ace (Dainippon-pharm., Osaka, Japan), the membrane was incubated with anti-phosphorylated ERK1/2 (pT202/pY204) (1:2000) in blocking solution. Horseradish peroxidase (HRP)-conjugated, anti-mouse antibody was used at a 1:10 000 dilution in Tween phosphate-buffered saline, followed by detection using SuperSignal (Pierce, Rockford, IL, USA). Total ERK levels were determined after stripping the membrane and probing with anti-total ERK1/2 antibody (1:2000), with HRP-conjugated anti-mouse immunoglobulin G as the secondary antibody. The optical densities of the bands on the film were quantified using densitometry.

Quantification of phosphorylated ERK2 (using ELISA)

Endothelium-denuded aortic tissues were suspended in an organ bath and incubated with 10 μM LPC for 15 min. After incubation, the preparations were exposed to 100 nM UK14,304 for 30 min. For experiments with inhibitors, tissues were pretreated with 10 μM genistein or 10 μM PD98059 for 20 min before the addition of LPC. These tissues were removed rapidly from the organ bath and rinsed with ice-cold Ca^{2+}-free KHS containing 1 mM SOV and 5 mM EDTA. They were then frozen in liquid N_2 and physically crushed to a fine powder in liquid N_2 using a Cryo-Press (Microtech Nichion, Chiba, Japan). Following lysation of these powder samples, phosphorylated ERK2 levels were lysated and then quantified using a Human/Mouse/Rat Phospho-ERK2 (T185/Y187) Surveyor IC immunoassay system (R&D Systems Inc., Minneapolis, MN, USA) according to the manufacturer's instructions.

Measurement of the expressions of the mRNA for GPR4 (using RT–PCR)

RNA was isolated by the guanidinium method. Briefly, in aortae carefully isolated from LETO and OLETF rats, the endothelium was removed by rubbing the intimal surface with a cotton swab (as described above). To confirm removal of endothelial cells, reverse transcription-polymerase chain reaction (RT–PCR) analysis of endothelial markers was performed using oligonucleotides specific for von Willebrand factor (vWF) (Kobayashi *et al*., 2005). Tissues were then homogenized in RNA buffer and the RNA was quantified by ultraviolet-absorbance spectrophotometry. For the RT–PCR analysis, first-strand cDNA was synthesized from total RNA using Oligo (dT) 20 and a ThermoScript RT–PCR System (Invitrogen Corp., Carlsbad, CA, USA), as described previously (Kanie *et al*., 2003; Matsumoto *et al*., 2003; Kobayashi *et al*., 2005). All primers were synthesized by Sigma-Genosys (St Louis, MO, USA). Individual sequences, PCR conditions and product sizes are shown in Table 1. To ensure that we were within the exponential phase of the semi-quantitative PCR reaction, the appropriate number of cycles was re-established for each set of samples. Control PCR

Table 1 PCR primers and PCR protocols

cDNA	*PCR primer sequences*	*PCR protocols*	*Product size (bp)*
GPR4	5′-CCTCTTCCCACCATCTCTC-3′ 5′-AGAGGAAGCCCACAAAGAC-3′	94°C/60 s 57°C/60 s 72°C/6O s 28 cycles	524
vWF	5′-GCGTGGCAGTGGTAGAGTA-3′ 5′-GGAGATAGCGGGTGAAATA-3′	94°C/60 s 56°C/60 s 72°C/6O s 25 cycles	261
GAPDH	5′-TCCCTCAAGATTGTCAGCAA-3′ 5′-AGATCCACAACGGATACATT-3′	94°C/60 s 54°C/60 s 72°C/60 s 21 cycles	308

Abbreviations: GAPDH, glyceraldehydes-3-phosphate dihydrogenase; GPR4, G-protein-coupled receptor 4; PCR, polymerase chain reaction; vWF, von Willebrand factor

Table 2 Values of various parameters in LETO and OLETF rats

Parameters	*LETO*	*OLETF*
Body weight (g)	561.7±11.3 (12)	678.1±42.5 (12)*
Plasma glucose (mg dl^{-1})	155.2±2.9 (12)	335.3±55.5 (12)**
Plasma cholesterol (mg dl^{-1})	100.5±1.8 (12)	210.6±28.4 (12)***
Plasma HDL (mg dl^{-1})	44.4±1.8 (12)	73.0±6.0 (12)***
Plasma LDL (mg dl^{1})	35.9±2.3 (12)	95.5±18.6 (12)**
Plasma triglyceride (mg dl^{-1})	93.8±6.8 (12)	380.5±65.2 (12)***
Plasma insulin (pg ml^{-1})	1512.7±156.1 (12)	1468.7±179.0 (12)
Plasma MDA (μM)	21.7±2.6 (10)	33.6±4.5 (10)*
Plasma SOD activity (%)	25.7±0.8 (12)	20.9±0.9 (12)***
Blood pressure (mm Hg)	112.4±1.8 (12)	135.4±4.3 (12)***

Abbreviations: HDL, high-density lipoprotein; LDL, low-density lipoprotein; LETO, Long–Evans Tokushima Otsuka; MDA, malondialdehyde; OLETF, Otsuka Long–Evans Tokushima Fatty; SOD, superoxide dismutase.
Number of determinations is shown within parentheses.
*$P<0.05$.
**$P<0.01$.
***$P<0.001$ vs LETO rats (ANOVA, followed by Bonferroni test).

reactions, in which the RT was omitted, were run simultaneously to check for successful removal of the genomic DNA. The PCR products so obtained were analysed on ethidium bromide-stained agarose (1.5%) gels, then quantified by scanning densitometry, with the amount of each product being normalized with respect to the amount of glyceraldehydes-3-phosphate dihydrogenase (GAPDH) product.

Reagents

Phenylmethylsulphonyl fluoride, AEBSF, aprotinin, EDTA, daidzein, genistein, leupeptin, L-α-lysophosphatidylcholine (palmitoyl) (LPC), NaF, SOV, Triton X-100, protease inhibitor cocktail and 5-bromo-6-[2-imidazolin-2-ylamino]-quinoxaline (UK14,304) were all purchased from Sigma Chemical Co. (St Louis, MO, USA), whereas ACh was from Daiichi Pharmaceuticals (Tokyo, Japan). PD98059 and tyrphostin A23 were from Calbiochem-Novabiochem Corporation (La Jolla, CA, USA). All drugs were dissolved in saline, except where otherwise noted. All concentrations are expressed as the final molar concentration of the base in the organ bath. HRP-linked secondary anti-mouse antibody was purchased from Promega (Madison, WI, USA), whereas antibodies against phosphorylated ERK1/2 (pT202/pY204) and ERK1/2 were obtained from BD Biosciences (San Jose, CA, USA).

Statistical analysis

Data are expressed as the mean±s.e.m. Contractile responses are expressed as a percentage of the response to 80 mM KCl. Multiple comparisons between treatment groups were performed by using an analysis of variance (ANOVA) followed by a Bonferroni test.

Results

General parameters

As demonstrated previously (Matsumoto *et al*., 2006a), at the time of the experiment, all OLETF rats (non-fasted) exhibited hyperglycaemia, their blood glucose concentrations being significantly higher than those of the age-matched non-diabetic control LETO rats (also non-fasted) (Table 2). The body weight of the OLETF rats was greater than that of LETO rats (Table 2). The plasma total cholesterol, triglyceride, HDL, LDL and MDA levels were all significantly higher in OLETF rats than in LETO rats, whereas the plasma insulin concentrations were similar in the two groups (Table 2). The plasma SOD activity was lower in OLETF rats than in LETO rats (Table 2). The systolic blood pressure of OLETF rats was higher than that of LETO rats (Table 2).

Effects of LPC on high-K^+-induced contractions in endothelium-denuded aortae from LETO and OLETF rats

Exposure of endothelium-denuded aortic strips to isotonic high K^+ (10–40 mM) led to a concentration-dependent rise in tension in age-matched LETO and OLETF rats, and there was no significant difference in sensitivity between the two groups (Figure 1a). At a concentration of 10 μM, LPC did not cause tension development, but it did significantly potentiate the high-K^+-induced contraction, the effect being most marked at 10–20 mM in both groups (Figure 1a). In particular, the LPC-induced potentiation of high-K^+-induced contraction was greater in OLETF rats than in LETO rats (Figure 1a).

Although 10 μM genistein, a PTK inhibitor, did not significantly inhibit the high-K^+-induced contraction in either LETO or OLETF rats (data not shown), the potentiating effect of LPC on this contraction was significantly inhibited by 10 μM genistein in both LETO and OLETF rats (Figure 1b and c). However, the potentiating effect of LPC on this contraction was not inhibited by 10 μM daidzein (an inactive isomer of genistein) in both the LETO and OLETF rats (Figure 1b and c). Such inhibitory effects of genistein on the LPC-induced enhancement of the high-K^+-induced contraction are consistent with our previous findings (Suenaga and Kamata, 2002, 2003).

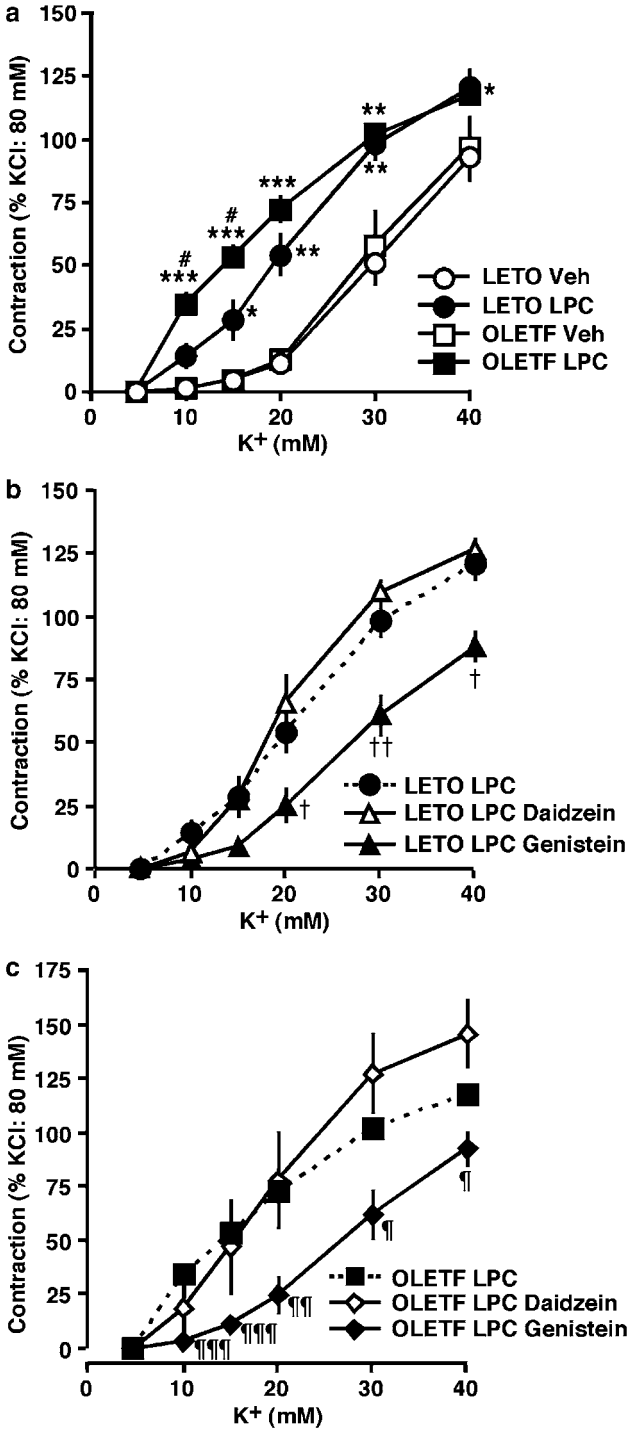

Figure 1 (**a**) Dose–response curves for high K^+ in the absence (vehicle; Veh) or presence of 10 μM LPC in endothelium-denuded aortae isolated from LETO and OLETF rats. Effects of the tyrosine kinase inhibitor genistein (10 μM) and its inactive isomer daidzein (10 μM) on the high-K^+-induced contraction in the presence of 10 μM LPC in endothelium-denuded aortae isolated from LETO (**b**) and OLETF (**c**) rats. Details are given under Methods. For comparison, the dose–response curves in the presence of LPC depicted in (**a**) are shown again in (**b**) and (**c**). Each data point represents the mean$\pm$s.e.m. from four or five experiments. $^*P<0.05$, $^{**}P<0.01$, $^{***}P<0.001$ vs corresponding Veh. $^{\#}P<0.05$ vs LPC-treated LETO. $^{\dagger}P<0.05$, $^{\dagger\dagger}P<0.01$ vs LPC-treated LETO. $^{\P}P<0.05$, $^{\P\P}P<0.01$, $^{\P\P\P}P<0.001$ vs LPC-treated OLETF (ANOVA followed by Bonferroni test).

Effects of LPC on UK14,304-induced contractions in endothelium-denuded aortae from LETO and OLETF rats

As shown previously (Suenaga and Kamata, 2002, 2003), LPC potentiates not only the contractile response induced in the endothelium-denuded rat aorta by high-K^+ but also that induced by UK14,304, a selective α_2-adrenoceptor agonist. We investigated the effect of LPC on UK14,304-induced contractions in both LETO and OLETF rats (Figure 2), then examined the effects of genistein, daidzein, tyrphostin A23 and PD98059 (a selective MEK inhibitor) on these LPC-modulated contractions (Figure 3). At concentrations of 10 nM (Figure 2a) and 30 nM (Figure 2b), LPC potentiated the UK14,304-induced contraction in a dose-dependent manner.

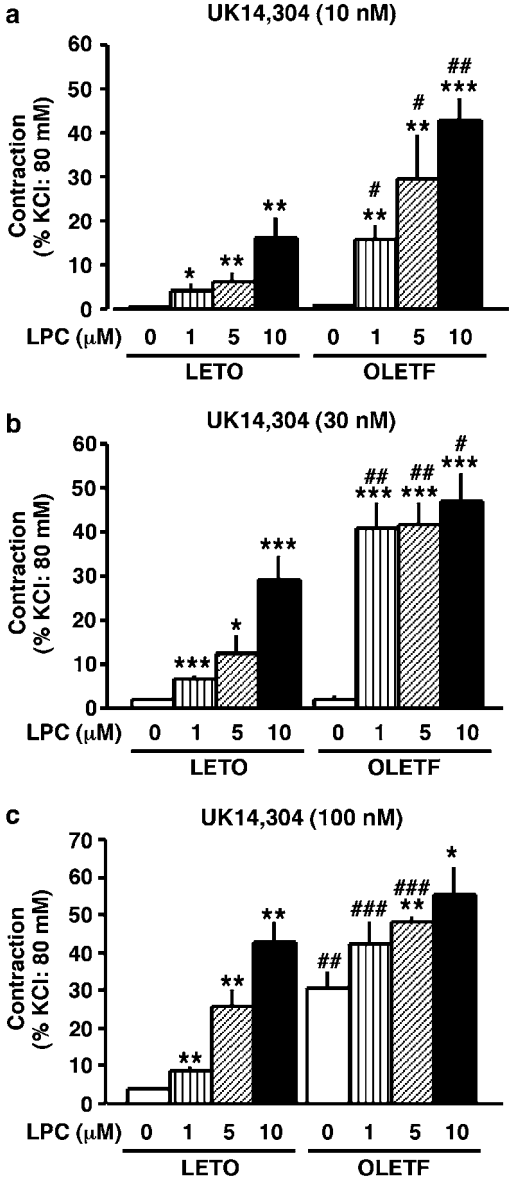

Figure 2 Effects of LPC on (**a**) 10 nM, (**b**) 30 nM or (**c**) 100 nM UK14,304-induced contraction. Details are given in Methods. Each column represents the mean$\pm$s.e.m. from four to eight experiments. $^*P<0.05$, $^{**}P<0.01$, $^{***}P<0.001$ vs corresponding Veh-treated group. $^{\#}P<0.05$, $^{\#\#}P<0.01$, $^{\#\#\#}P<0.001$ vs same concentration of LPC in LETO (ANOVA followed by Bonferroni test).

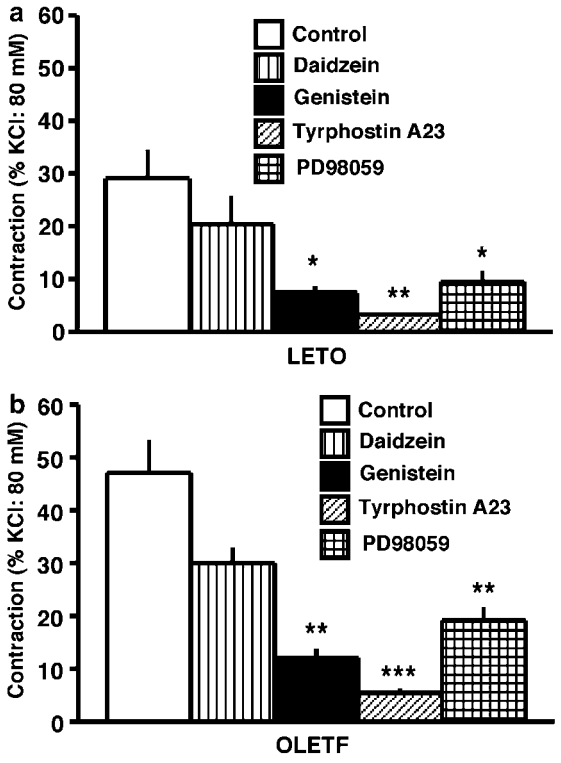

Figure 3 Effects of two tyrosine kinase inhibitors, genistein (10 μM) and tyrphostin A23 (50 μM), together with the effects of daidzein (10 μM, the inactive isomer of genistein) and PD98059 (10 μM, a MEK inhibitor) on 30 nM UK14,304-induced contraction in the presence of 10 μM LPC in endothelium-denuded aortae isolated from LETO (**a**) and OLETF (**b**) rats. Details are given in Methods. For comparison, the 30 nM UK14,304-induced contraction in the presence of 10 μM LPC depicted in Figure 2b is shown again (Control). Each column represents the mean$\pm$s.e.m. from four to eight experiments. *$P<0.05$, **$P<0.01$, ***$P<0.001$ vs Control (ANOVA followed by Bonferroni test).

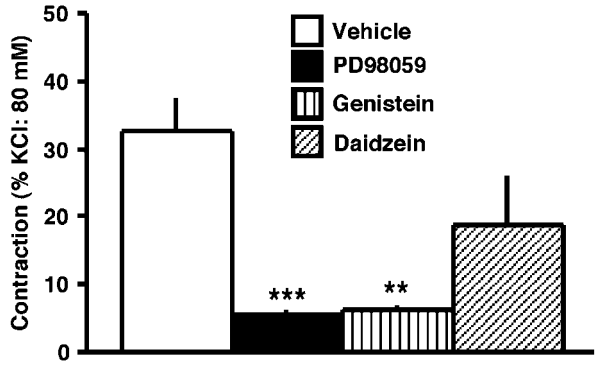

Figure 4 Effects of the tyrosine kinase inhibitor genistein (10 μM), together with those of daidzein (10 μM, the inactive isomer of genistein) and PD98059 (10 μM, a MEK inhibitor) on 100 nM UK14,304-induced contraction in endothelium-denuded aortae isolated from OLETF rats. Details are given in Methods. For comparison, the 100 nM UK14,304-induced contraction depicted in Figure 2c is shown again (Control). Each column represents the mean$\pm$s.e.m. from four to eight experiments. **$P<0.01$, ***$P<0.001$ vs Control (ANOVA followed by Bonferroni test).

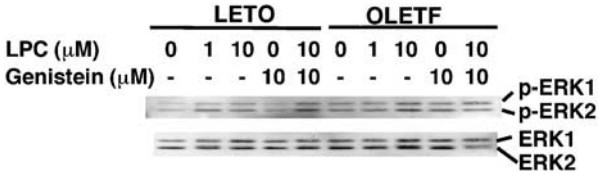

Figure 5 LPC-induced ERK phosphorylation in endothelium-denuded aortae from LETO and OLETF rats. Typical blots of phosphorylated ERK (p-ERK) and total ERK (ERK) under various conditions. Details are given in Methods.

The magnitude of this potentiation was significantly greater in OLETF rats than in LETO rats, not only at a high concentration (i.e. 10 μM) but also at lower concentrations (i.e. 1 and 5 μM) of LPC (Figure 2). Genistein (10 μM), tyrphostin A23 (50 μM) and PD98059 (10 μM), but not daidzein (10 μM), significantly inhibited the 10 μM LPC-induced potentiation of the 30 nM UK14,304-induced response in both OLETF and LETO aortae (Figure 3). At a concentration of 100 nM UK14,304 (Figure 2c), the UK14,304-induced contraction in the absence of LPC was significantly greater in the OLETF than in the LETO group. LPC augmented the 100 nM UK14,304-induced contraction in both LETO and OLETF groups, just as it did in the 10 and 30 nM UK14,304-induced contractions. The 100 nM UK14,304-induced contraction in endothelium-denuded aortae from OLETF rats was significantly inhibited by genistein (10 μM) and PD98059 (10 μM), but not by daidzein (10 μM) (Figure 4).

Effects of LPC on ERK activation in endothelium-denuded aortae from LETO and OLETF rats

The present data (Figures 3 and 4) and previous findings suggest that the ERK pathway modulates the effects of several vasoconstrictors on vascular smooth muscle (Roberts, 2001; Suenaga and Kamata, 2003). As shown in Figure 5 and Table 3, LPC-induced ERK2 activation occurred in a concentration-dependent manner in LETO rats, and this increased activity was suppressed by genistein (10 μM) treatment. Interestingly, the basal (vehicle-treated) level of ERK2 activity was greater in OLETF rats than in LETO rats, and this ERK2 activity tended to be (not significantly) further increased by LPC treatment. These vehicle- and/or LPC (10 μM)-treated ERK2 activity levels in OLETF rats were significantly decreased by genistein (10 μM) treatment.

Effects of LPC on UK14,304-induced ERK2 activation in endothelium-denuded aortae from LETO and OLETF rats

Recent studies have demonstrated that in several vessels, α_2-adrenoceptor-mediated vasoconstriction occurs through activation of ERK2 (Roberts, 2001, 2004; Bhattacharya and Roberts, 2003). Levels of phosphorylated ERK2 were measured by enzyme-linked immunosorbent assay (ELISA) (Figure 6). Interestingly, the ERK2 phosphorylation level following vehicle treatment was greater in OLETF rats than in LETO rats (Figure 6a). The level of ERK2 phosphorylation was increased by treatment with 100 nM UK14,304 to a similar extent in both LETO and OLETF (Figure 6b). This effect of UK14,304 was inhibited by 10 μM PD98059 in both groups (data not shown). The UK14,304-induced ERK2

Table 3 Changes in the levels of phosphorylated and total ERK1/2 in endothelium-denuded aortae from LETO and OLETF rats

	LETO		*OLETF*	
	Phospho-ERK1	*Total ERK1*	*Phospho-ERK1*	*Total ERK1*
Vehicle	100%	100%	138.1±22.2% (4)	137.4±7.6% (4)**
LPC (1 μM)	122.6±9.9% (4)	111.8±8.6% (4)	160.8±18,6% (4)	116.0±4.6% (4)
LPC (10 μM)	131.5±22.1% (4)	113.4±15.2% (4)	167.6±36.9% (4)	114.5±18.0% (4)
Genistein (10 μM)	154.9±65.1% (3)	99.0±16.3% (3)	107.7±36.7% (3)	95.6±7.1% (3)¶
Genistein (10 μM)+LPC (10 μM)	99.9±29.0%(4)	108.9±11.4% (4)	103.4±25.3% (4)	108.3±13.6% (4)
	LETO		*OLETF*	
	Phospho-ERK2	*Total ERK2*	*Phospho-ERK2*	*Total ERK2*
Vehicle	100%	100%	148.1±11.3% (4)**	116.7±13.2% (4)
LPC (1 μM)	123.0±8.8% (4)*	104.6±8.8% (4)	166.1±4.9% (4)	108.4±13.4% (4)
LPC (10 μM)	179.8±19.6% (4)‡**	108.7±8.0% (4)	192.5±16.6% (4)	113.8±14.2% (4)
Genistein (10 μM)	87.3±6.6% (3)	104.6±13.5% (3)	75.7±43% (3)¶¶	91.2±12.3% (3)
Genistein (10 μM)+LPC (10 μM)	82.6±9.3% (4)$^{\#\#}$	106.1±20.1% (4)	109.1±16.6% (4)†	101.6±6.9% (4)

Abbreviations: ERK, extracellular signal-regulated kinase; LETO, Long–Evans Tokushima Otsuka; LPC, lysophosphatidylcholine; OLETF, Otsuka Long–Evans Tokushima Fatty.
Phosphorylated (phospho-ERK1/2) and total ERK1/2 levels were determined by Western blotting, as outlined in the Methods section. Densitometoric analysis of the bands on the immunoblots was carried out and the results are expressed as a percentage of the vehicle-treated LETO level.
Number of determinations is shown within parentheses.
*$P<0.05$.
**$P<0.01$ vs vehicle-treated LETO.
$^{\#\#}P<0.01$ vs LPC (10 μM)-treated LETO.
$^{\P}P<0.05$.
$^{\P\P}P<0.01$ vs vehicle-treated OLETF.
$^{\dagger}P<0.05$ vs LPC (10 μM)-treated OLETF.
$^{\ddagger}P<0.05$ vs LPC (1 μM)-treated LETO.
ANOVA, followed by Bonferroni test.

phosphorylation was significantly increased in the presence of 10 μM LPC in the LETO group but not in the OLETF group (Figure 6b). Treatment with PD98059 (10 μM) or genistein (10 μM) significantly reduced the LPC-enhanced ERK2 phosphorylation level in both LETO and OLETF groups (data not shown).

Contractile responses to a tyrosine phosphatase inhibitor in endothelium-denuded aortae from LETO and OLETF rats

The PTK pathway contributes to the signalling processes that lead to contraction in vascular smooth muscle (Hollenberg, 1994). Moreover, as described above, PTK is involved in the LPC-induced enhancement of contractile responses ((Suenaga and Kamata, 2002; Figures 1, 3 and 4). To investigate whether this signalling process might differ between endothelium-denuded aortae from LETO and those from OLETF rats, we performed a series of experiments in which SOV (a tyrosine phosphatase inhibitor) was added cumulatively to aortic strips (Figure 7). The SOV (10 μM$\sim$3 mM)-induced concentration-dependent contractile response was significantly greater in OLETF rats than in age-matched LETO rats (Figure 7a), and this enhanced response was significantly inhibited by 10 μM genistein, but not by 10 μM daidzein (Figure 7b and c). Moreover, these SOV-induced contractions were augmented by 10 μM LPC in both groups (notably, this augmentation by LPC was greater in OLETF than in LETO) (Figure 8a). This LPC-induced enhancement was suppressed by 10 μM PD98059 and 10 μM genistein, but not by 10 μM daidzein in both OLETF and LETO (Figure 8b and c).

Expression of the mRNA for GPR4 in vascular smooth muscle cells from LETO and OLETF rats

Using RT–PCR on the total RNA isolated from the vascular smooth muscle cells or endothelial cells of aortae from LETO and OLETF rats, we found the following. RT–PCR analysis of endothelial markers was performed using a specific oligonucleotide. After 25 PCR cycles, positive expression for vWF was detected only in the total RNA from endothelial cells, not in that from smooth muscle cells (Figure 9a). The expression of GAPDH mRNA in vascular smooth muscle cells showed no difference between aortae from LETO and OLETF rats (Figure 9b). However, the expression of GPR4 mRNA in vascular smooth muscle cells was significantly greater in the OLETF group than in the LETO group (Figure 9b and c).

Discussion

In the present study, we demonstrated that in OLETF rats, a model of type II diabetes, the LPC-induced potentiation of contractile responses in the endothelium-denuded aorta is greater than that seen in LETO rats, and that the mechanisms underlying this abnormality may be related to increases in PTKs and ERK activities and/or to an upregulation of GPR4, a putative LPC receptor.

It is widely known that the PTK pathway and/or ERK pathway are implicated in a wide range of cellular functions, including proliferation, migration, survival and vascular contraction (Hollenberg, 1994; Touyz and Schiffrin, 2000; Roberts, 2001). LPC has been shown to have a mitogenic effect on vascular smooth muscle cells (Chen *et al*., 1995).

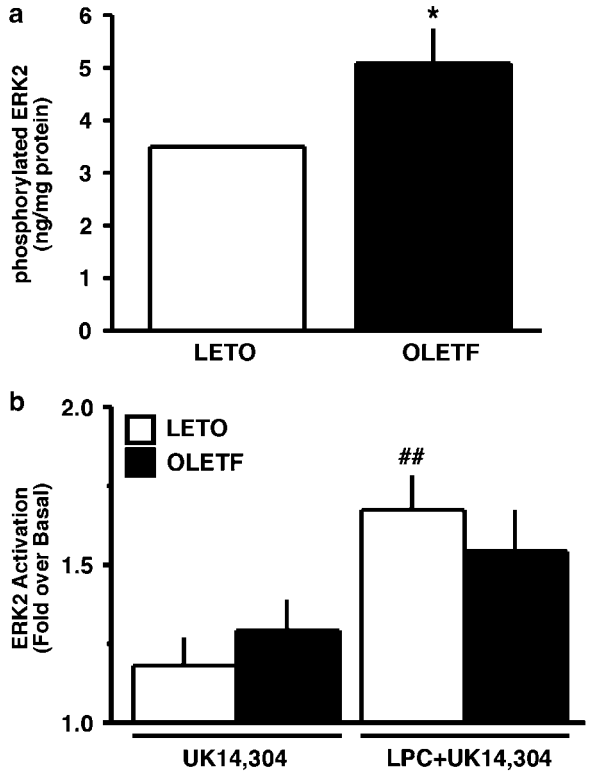

Figure 6 Quantification of phosphorylated ERK2 of (**a**) vehicle (basal), (**b**) UK14,304 or LPC plus UK14,304-treated endothelium-denuded aortae from LETO and OLETF rats. Endothelium-denuded aortic tissues were suspended in an organ bath and incubated with 10 μM LPC for 15 min. After incubation, the preparations were exposed to 100 nM UK14,304 for 30 min. Details are given in Methods. Each column represents the mean$\pm$s.e.m. from five experiments. *$P<0.05$ vs LETO group. $^{\#\#}P<0.01$ vs UK14,304-treated LETO group (ANOVA followed by Bonferroni test).

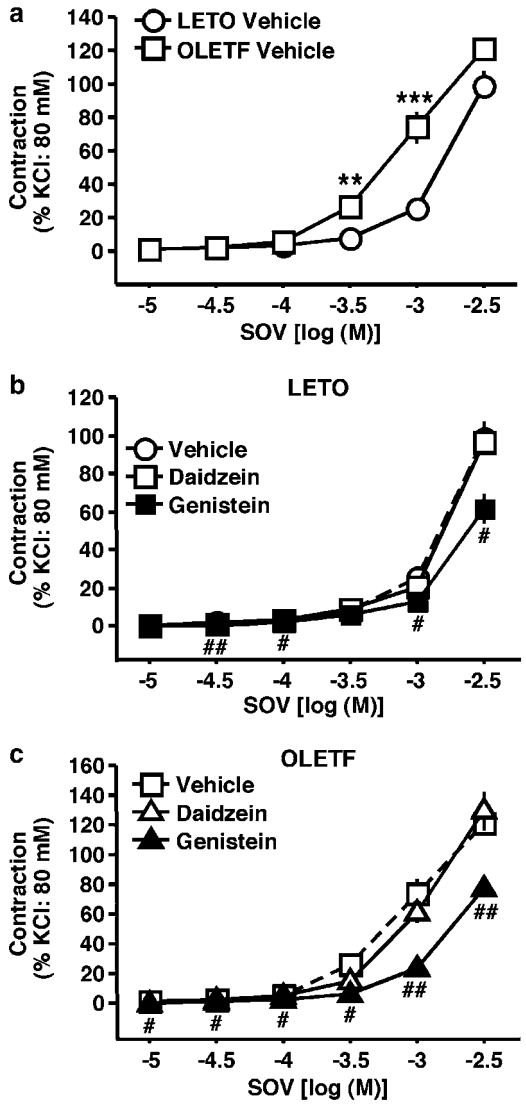

Figure 7 Contractions induced by SOV in endothelium-denuded aortae from LETO and OLETF rats. (**a**) Dose–response curves for SOV. Effects of 10 μM daidzein or 10 μM genistein on SOV-induced contraction in endothelium-denuded aortae from LETO (**b**) and OLETF (**c**) rats. Details are given in Methods. For comparison, the vehicle-treated dose–response curves for SOV depicted in (**a**) are shown again in (**b**) and (**c**). Each data point represents the mean$\pm$s.e.m. from three to six experiments. **$P<0.01$, ***$P<0.001$ vehicle-treated LETO vs vehicle-treated OLETF (**a**). $^{\#}P<0.05$, $^{\#\#}P<0.01$ vs vehicle-treated group (**b**, **c**). (ANOVA followed by Bonferroni test).

Also, activation of membrane or cytoplasmic PTKs may play a key role in LPC-induced mitogenic signalling responses (Bassa *et al*., 1999). Indeed, our previous studies (Suenaga and Kamata, 2002, 2003) demonstrated that LPC potentiates contractile responses in the endothelium-denuded aorta via activation of PTKs and/or ERK, which in turn regulates Ca^{2+} influx. In the present study, our first finding was that the potentiating effects of LPC on high-K^+- (Figure 1) and UK14,304- (Figure 3) induced contractions of the endothelium-denuded aorta were inhibited by 10 μM genistein. The same concentration (10 μM) of daidzein, a genistein analogue that is inactive as a PTK inhibitor (Akiyama *et al*., 1987), did not inhibit the LPC effect at all (Figures 1, 3 and 4). Moreover, we previously demonstrated that LPC increases the tyrosine phosphorylation of several proteins and that these effects were inhibited by genistein at a concentration (10 μM) that also attenuated the LPC-induced potentiation of the contractile responses to high-K^+ and UK14,304 (Suenaga and Kamata, 2002). Taken together, these previous and present results suggest that the inhibition of the LPC-induced potentiating effect produced by genistein is probably due to an attenuation of PTK activity. Our finding that LPC did not potentiate the UK14,304-induced contraction in the presence of 50 μM tyrphostin A23 (a non-flavone PTK inhibitor) (Figure 3) supports this conclusion. Recent studies have demonstrated that in several vessels, α_2-adrenoceptor-mediated vasoconstriction occurs through activation of ERK2 (Ozaki *et al*., 1999; Roberts, 2001, 2004; Bhattacharya and Roberts, 2003). In the present study, we found that 10 μM PD98059 markedly attenuated contraction and ERK2 activity induced by UK14,304. Moreover, the potentiating effects produced by LPC on UK14,304-induced contraction and ERK2 activity were also inhibited by 10 μM PD98059. These results suggest that both the UK14,304-induced contractile response and its modulation by LPC may be regulated via the ERK pathway.

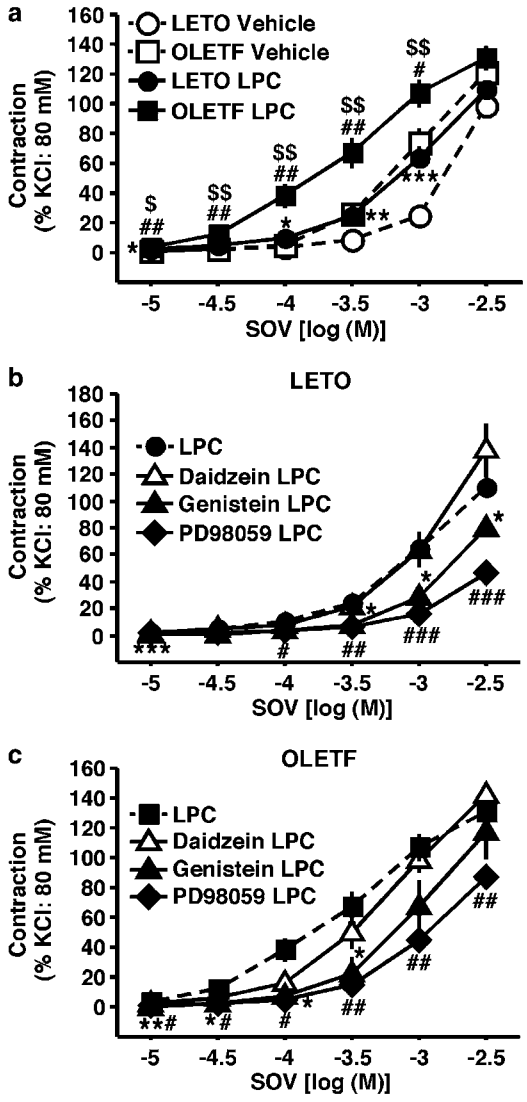

Figure 8 Contractions induced by SOV in the presence of 10 μM LPC in endothelium-denuded aortae from LETO and OLETF rats. (**a**) Dose–response curve for SOV in the presence of LPC. Effects of 10 μM daidzein, 10 μM genistein or 10 μM PD98059 on SOV-induced contraction in endothelium-denuded aortae from LETO (**b**) and OLETF (**c**) rats. Details are given in Methods. For comparison, the vehicle-treated dose–response curves for SOV depicted in Figure 7a are shown again in (**a**), and the LPC-treated dose–response curves for SOV depicted in (**a**) are shown again in (**b**) and (**c**) (LPC). Each data point represents the mean$\pm$s.e.m. from three to six experiments. In (**a**), $^{*}P<0.05$, $^{**}P<0.01$, $^{***}P<0.001$, vehicle-treated LETO vs LPC-treated LETO. $^{\#}P<0.05$, $^{\#\#}P<0.01$, vehicle-treated OLETF vs LPC-treated OLETF. $^{\$}P<0.05$, $^{\$\$}P<0.01$, LPC-treated LETO vs LPC-treated OLETF. In (**b** and **c**), $^{*}P<0.05$, $^{**}P<0.01$, $^{***}P<0.001$, genistein + LPC-treated group vs LPC-treated group. $^{\#}P<0.05$, $^{\#\#}P<0.01$, $^{\#\#\#}P<0.001$, PD98059 + LPC-treated group vs LPC-treated group. (ANOVA followed by Bonferroni test).

In the present study, we examined whether the LPC-induced contractile responses and PTK and ERK activities were altered in the endothelium-denuded aortae from OLETF rats. The results suggest that the additional effect of LPC on ERK2 activation was smaller in aortae from the OLETF group than in those from the LETO group because the basal ERK2 phosphorylation was already increased by LPC-mediated

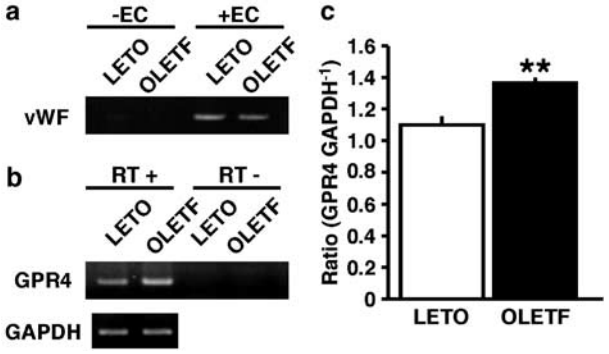

Figure 9 RT–PCR assays of GPR4 mRNA expression in endothelium-denuded aortae isolated from LETO and OLETF rats. Details are given in Methods. (**a**) To verify successful removal of endothelium, vWF (an endothelial marker) was investigated. +EC, endothelium-intact preparation; −EC, endothelium-denuded preparation. (**b**) Expression of mRNAs for GPR4 and GAPDH in aortic smooth muscle cells. RT+, reverse transcription; RT−, no reverse transcription. (**c**) Quantitative analysis of expression of GPR4 mRNAs in aortic smooth muscle cells from LETO and OLETF rats. Values are each the mean$\pm$s.e.m. of four determinations (GPR4 GAPDH^{-1}). $^{**}P<0.01$ *vs* LETO (ANOVA followed by Bonferroni test).

signalling or other factors in diabetic states. The increased basal ERK2 activity may be responsible for the increased UK14,304-induced contraction in the OLETF group, Moreover, the involvement of PTK is further supported by the observed contractile effects of SOV in the endothelium-denuded rat aorta (Figures 7 and 8). SOV has previously been shown, by Filipeanu *et al*. (1995), to produce a contraction that is sensitive to genistein. Here, we found that both the SOV-induced contraction and its modulation by LPC were inhibited by the 10 μM genistein, but not by 10 μM daidzein (Figures 7 and 8). These results suggest that the magnitude of a protein-tyrosine-phosphorylation-mediated contraction is determined by the balance between the activities of PTK and protein tyrosine phosphatase in smooth muscle cells. The SOV-induced contraction was greater in OLETF group than in the LETO group (Figure 7). Moreover, the SOV-induced contraction was augmented by 10 μM LPC in both groups (but more markedly in OLETF) (Figure 8a). These LPC-induced enhancements of the SOV-induced contraction were suppressed by 10 μM PD98059. Taken together, these results strongly suggest that both the increased UK14,304-induced contraction and the LPC-induced augmentation of contractions observed in the OLETF rat aorta may be attributable to increases in the activities of PTKs or ERK.

Recent evidence suggests that two cloned orphan G-protein-coupled receptors, GPR4 and G2A, may serve as specific LPC receptors in several cells (Xu, 2002). As well as monocytes/macrophages, vascular endothelial and smooth muscle cells play an important role in atherogenesis. However, Rikitake *et al*. (2002) found that G2A was not detected in these cells, but was expressed predominantly by macrophages within atherosclerotic lesions. On the other hand, Lum *et al*. (2003) found that GPR4 was expressed at a low level in human brain microvascular cells and that this expression was increased by either tumour necrosis factor-α (TNF-α) or H_2O_2. By contrast, a high basal GPR4 mRNA level was found in human dermal microvascular endothelial cells,

and this was not further increased by either TNF-α or H_2O_2 (Lum *et al*., 2003). Another LPC receptor, G2A, was not detected in either endothelial cell type (Lum *et al*., 2003). A receptor expression regulated by physiological and pathological conditions could play an important role in controlling LPC-induced effects (Xu, 2002). In the present study, the GPR4 expression was significantly greater in endothelial-denuded aortae from OLETF rats compared to those from LETO rats (Figure 9). These results suggest that an increased GPR4 expression in smooth muscle cells, but not endothelial cells, may partly explain the hyper-reactivity to LPC and the increased basal ERK2 activity seen in the diabetic state. Although the activation of LPC receptors induced ERK activation in several cells (Xu, 2002), it has been suggested that the actions of LPC may be mediated not only by receptors but also by non-receptors (Xu, 2002). Whether the observed GPR4 upregulation contributes to the LPC-mediated modulation of contractile responses and the increased ERK2 activity, in diabetic states, may become clear when pharmacological antagonists of LPC receptors or a GPR4 antibody become commercially available.

Although the mechanism underlying the above differences in the activities of PTK and ERK between diabetic and control rats remains unclear, metabolic and/or hormonal alterations might be involved. Previous studies have shown that high glucose and TNF-α levels can induce activation of PTK and/or ERK signalling pathways (Li *et al*., 2003; Schaeffer *et al*., 2003). Moreover, native and modified lipoproteins activate these signalling pathway (Velarde *et al*., 2001). OLETF rats are characterized by late-onset hyperglycaemia and by a mild and chronic course of diabetes, as well as by mild obesity (Kawano *et al*., 1992). In addition, our studies demonstrate that OLETF rats have metabolic abnormalities such as increases in plasma glucose, triglyceride and cholesterol. Thus, it is possible that the observed abnormalities in PTK/ERK activities may be due to changes in the plasma levels of the above parameters. However, to establish causal relationships will require further research focusing, for example, on the time course of the changes, both in the levels of these parameters and in PTK and/or ERK activities in diabetic states.

Published evidence indicates that the circulating levels of several forms of modified LDL, including oxidative modified LDL, are elevated in the plasma in diabetes (Bagdade *et al*., 1990). The level of LDL oxidation is known to be related to the severity of coronary atherosclerosis (Regnstrom *et al*., 1992) and is believed to be determined not only by antioxidants (as inhibitory factors) but also by lipid peroxides (as stimulating factors). Moreover, Takahara *et al*. (1997) suggested that LPC levels in the lipoprotein fraction, which reflect oxidative modification of the lipoproteins, are at least a possible atherogenic marker for the biological activity of lipoprotein in diabetic patients. In our OLETF rats: (i) the plasma LDL level was increased, (ii) plasma SOD activity (antioxidant system) was decreased and (iii) the plasma MDA level (lipid peroxides) was increased. These results suggest that an enhanced level of LPC generation may be present in our diabetic model. Although the plasma level of LPC was not directly measured in the present study, this hypothesis is supported by the finding that the LPC level is increased in type II diabetic patients (Rabini *et al*., 1994; Takahara *et al*., 1997; Shi *et al*., 1999). Further studies are required to investigate this point. Baumgart *et al*. (1999) demonstrated that in normal coronary arteries, α_2 (but not α_1)-adrenoceptor activation reduces coronary blood flow via microvascular constriction. They further showed that both α_1- and α_2-adrenoceptor-mediated epicardial and microvascular constriction are augmented by atherosclerosis and can induce myocardial ischaemia. This suggests that the involvement of α_2-adrenoceptors may be a target for more specific drug therapy. The above evidence and the present findings suggest that an alteration in α_2-mediated vasoconstriction and its modulation by LPC may contribute both to the cardiovascular disease associated with type II diabetes and to atherosclerotic disorders.

In conclusion, we found that LPC-mediated modulation of contractile responses was greater in aortae from type II diabetic rats (OLETF) than in those from control (LETO) rats, and that this abnormality may be attributable to increased PTK/ERK activity and/or to GPR4 upregulation. Future research into vascular signalling mechanisms should continue to focus on physiological and therapeutic means of inhibiting the LPC signal-transduction cascade in the vascular pathology of diabetics.

Acknowledgements

We thank E Arai and Y Nasu for technical help. We also thank Otsuka Pharmaceutical for providing LETO and OLETF rats. This study was supported in part by the Ministry of Education, Culture, Sports, Science and Technology, Japan, and by the Promotion and Mutual Aid Cooperation for Private Schools of Japan.

Conflict of interest

The authors state no conflict of interest.

References

Akiyama T, Ishida J, Nakagawa S, Ogawara H, Watanabe S, Itoh N *et al*. (1987). Genistein, a specific inhibitor of tyrosine-specific protein kinases. *J Biol Chem* **262**: 5592–5595.

Bassa BV, Roh DD, Vaziri ND, Kirschenbaum MA, Kamanna VS (1999). Lysophosphatidylcholine activates mesangial cell PKC and MAP kinase by PLCgamma-1 and tyrosine kinase-Ras pathways. *Am J Physiol* **277**: F328–F337.

Bagdade JD, Buchanan WE, Kuusi T, Taskinen MR (1990). Persistent abnormalities in lipoprotein composition in noninsulin-dependent diabetes after intensive insulin therapy. *Arteriosclerosis* **10**: 232–239.

Baumgart D, Haude M, Gorge G, Liu F, Ge J, Grosse-Eggebrecht C *et al*. (1999). Augmented alpha-adrenergic constriction of atherosclerotic human coronary arteries. *Circulation* **99**: 2090–2097.

Bhattacharya B, Roberts RE (2003). Enhancement of alpha2-adrenoceptor-mediated vasoconstriction by the thromboxane-mimetic U46619 in the porcine isolated ear artery: role of the ERK-MAP kinase signal transduction cascade. *Br J Pharmacol* **139**: 156–162.

Chen Y, Morimoto S, Kitano S, Koh E, Fukuo K, Jiang B *et al*. (1995). Lysophosphatidylcholine causes Ca^{2+} influx, enhanced DNA synthesis and cytotoxicity in cultured vascular smooth muscle cells. *Atherosclerosis* **112**: 69–76.

De Vriese AS, Verbeuren TJ, Van De Voorde J, Lameire NH, Vanhoutte PM (2000). Endothelial dysfunction in diabetes. *Br J Pharmacol* **130**: 963–974.

Filipeanu CM, Brailoiu E, Huhurez G, Slatineanu S, Baltatu O, Branisteanu DD (1995). Multiple effects of tyrosine kinase inhibitors on vascular smooth muscle contraction. *Eur J Pharmacol* **281**: 29–35.

Friedewald WT, Levy RI, Fredrickson DS (1972). Estimation of the concentration of low-density lipoprotein cholesterol in plasma, without use of the preparative ultracentrifuge. *Clin Chem* **18**: 499–502.

Hollenberg MD (1994). Tyrosine kinase pathways and the regulation of smooth muscle contractility. *Trends Pharmacol Sci* **15**: 108–114.

Kamata K, Nakajima M (1998). Ca^{2+} mobilization in the aortic endothelium in streptozotocin-induced diabetic and cholesterol-fed mice. *Br J Pharmacol* **123**: 1509–1516.

Kanie N, Matsumoto T, Kobayashi T, Kamata K (2003). Relationship between peroxisome proliferators-activated receptors (PPAR alpha and PPAR gamma) and endothelial dependent relaxation in streptozotocin-induced diabetic rats. *Br J Pharmacol* **140**: 23–32.

Kawano K, Hirashima T, Mori S, Saitoh Y, Kurosumi M, Natori T (1992). Spontaneous long-term hyperglycemic rat with diabetic complications. Otsuka Long–Evans Tokushima Fatty (OLETF) strain. *Diabetes* **41**: 1422–1428.

Kobayashi T, Kaneda A, Kamata K (2003). Possible involvement of IGF-1 receptor and IGF-binding protein in insulin-induced enhancement of noradrenaline response in diabetic rat aorta. *Br J Pharmacol* **140**: 285–294.

Kobayashi T, Matsumoto T, Kamata K (2000). Mechanisms underlying the chronic pravastatin treatment-induced improvement in the impaired endothelium-dependent aortic relaxation seen in streptozotocin-induced diabetic rats. *Br J Pharmacol* **131**: 231–238.

Kobayashi T, Matsumoto T, Kamata K (2005). IGF-I-induced enhancement of contractile response in organ-cultured aortae from diabetic rats is mediated by sustained thromboxane A2 release from endothelial cells. *J Endocrinol* **186**: 367–376.

Kobayashi T, Taguchi K, Yasuhiro T, Matsumoto T, Kamata K (2004). Impairment of PI3-K/Akt pathway underlies attenuated endothelial function in aorta of type 2 diabetic mouse model. *Hypertension* **44**: 956–962.

Kugiyama K, Kerns SA, Morrisett JD, Roberts R, Henry PD (1990). Impairment of endothelium-dependent arterial relaxation by lysolecithin in modified low-density lipoproteins. *Nature* **344**: 160–162.

Li M, Mossman BT, Kolpa E, Timblin CR, Shukla A, Taatjes DJ *et al*. (2003). Age-related differences in MAP kinase activity in VSMC in response to glucose or TNF-alpha. *J Cell Physiol* **197**: 418–425.

Lum H, Qiao J, Walter RJ, Huang F, Subbaiah PV, Kim KS *et al*. (2003). Inflammatory stress increases receptor for lysophosphatidylcholine in human microvascular endothelial cells. *Am J Physiol Heart Circ Physiol* **285**: H1786–H1789.

Luscher TF, Creager MA, Beckman JA, Cosentino F (2003). Diabetes and vascular disease: pathophysiology, clinical consequences, and medical therapy: Part II. *Circulation* **108**: 1655–1661.

Matsumoto T, Kobayashi T, Kamata K (2003). Alterations in EDHF-type relaxation and phosphodiesterase activity in mesenteric arteries from diabetic rats. *Am J Physiol Heart Circ Physiol* **285**: H283–H291.

Matsumoto T, Kobayashi T, Kamata K (2006a). Mechanisms underlying the impaired EDHF-type relaxation response in mesenteric arteries from Otsuka Long–Evans Tokushima Fatty (OLETF) rats. *Eur J Pharmacol* **538**: 132–140.

Matsumoto T, Kobayashi T, Wakabayashi K, Kamata K (2005). Cilostazol improves endothelium-derived hyperpolarizing factor-type relaxation in mesenteric arteries from diabetic rats. *Am J Physiol Heart Circ Physiol* **289**: H1933–H1940.

Matsumoto T, Miyamori K, Kobayashi T, Kamata K (2006b). Specific impairment of endothelium-derived hyperpolarizing factor-type relaxation in mesenteric arteries from streptozotocin-induced diabetic mice. *Vasc Pharmacol* **44**: 450–460.

Matsumoto T, Sato A, Suenaga H, Kobayashi T, Kamata K (2004a). Modulations of shear stress-induced contractile responses and agonist-induced vasodilation in hypercholesterolemic rats. *Atherosclerosis* **175**: 31–38.

Matsumoto T, Wakabayashi K, Kobayashi T, Kamata K (2004b). Alterations in vascular endothelial function in the aorta and mesenteric artery in type II diabetic rats. *Can J Physiol Pharmacol* **82**: 175–182.

Mcintyre TM, Zimmerman GA, Prescott SM (1999). Biologically active oxidized phospholipids. *J Biol Chem* **274**: 25189–25192.

Ozaki H, Ishii K, Arai H, Kume N, Kita T (1999). Lysophosphatidylcholine activates mitogen-activated protein kinases by a tyrosine kinase-dependent pathway in bovine aortic endothelial cells. *Atherosclerosis* **143**: 261–266.

Rabini RA, Galassi R, Fumelli P, Dousset N, Solera ML, Valdiguie P *et al*. (1994). Reduced Na(+)-K(+)-ATPase activity and plasma lysophosphatidylcholine concentrations in diabetic patients. *Diabetes* **43**: 915–919.

Regnstrom J, Nilsson J, Tornvall P, Landou C, Hamsten A (1992). Susceptibility to low-density lipoprotein oxidation and coronary atherosclerosis in man. *Lancet* **339**: 1183–1186.

Rikitake Y, Hirata K, Yamashita T, Iwai K, Kobayashi S, Itoh H *et al*. (2002). Expression of G2A, a receptor for lysophosphatidylcholine, by macrophages in murine, rabbit, and human atherosclerotic plaques. *Arterioscler Thromb Vasc Biol* **22**: 2049–2053.

Roberts RE (2001). Role of the extracellular signal-regulated kinase (Erk) signal transduction cascade in alpha(2) adrenoceptor-mediated vasoconstriction in porcine palmar lateral vein. *Br J Pharmacol* **133**: 859–866.

Roberts RE (2004). The role of Rho kinase and extracellular regulated kinase-mitogen-activated protein kinase in alpha2-adrenoceptor-mediated vasoconstriction in the porcine palmar lateral vein. *J Pharmacol Exp Ther* **311**: 742–747.

Schaeffer G, Levak-Frank S, Spitaler MM, Fleischhacker E, Esenabhalu VE, Wagner AH *et al*. (2003). Intercellular signaling within vascular cells under high D-glucose involves free radical-triggered tyrosine kinase activation. *Diabetologia* **46**: 773–783.

Shi AH, Yoshinari M, Wakisaka M, Iwase M, Fujishima M (1999). Lysophosphatidylcholine molecular species in low density lipoprotein of type 2 diabetes. *Horm Metab Res* **31**: 283–286.

Suenaga H, Kamata K (1998). Lysophosphatidylcholine potentiates vascular contractile responses by enhancing vasoconstrictor-induced increase in cytosolic free Ca^{2+} in rat aorta. *Eur J Pharmacol* **361**: 217–226.

Suenaga H, Kamata K (2002). Lysophosphatidylcholine potentiates vascular contractile responses in rat aorta via activation of tyrosine kinase. *Br J Pharmacol* **135**: 789–799.

Suenaga H, Kamata K (2003). Lysophosphatidylcholine activates extracellular-signal-regulated protein kinase and potentiates vascular contractile responses in rat aorta. *J Pharmacol Sci* **92**: 348–358.

Takahara N, Kashiwagi A, Nishio Y, Harada N, Kojima H, Maegawa H *et al*. (1997). Oxidized lipoproteins found in patients with NIDDM stimulate radical-induced monocyte chemoattractant protein-1 mRNA expression in cultured human endothelial cells. *Diabetologia* **40**: 662–670.

Touyz RM, Schiffrin EL (2000). Signal transduction mechanisms mediating the physiological and pathophysiological actions of angiotensin II in vascular smooth muscle cells. *Pharmacol Rev* **52**: 639–672.

Velarde V, Jenkins AJ, Christopher J, Lyons TJ, Jaffa AA (2001). Activation of MAPK by modified low-density lipoproteins in vascular smooth muscle cells. *J Appl Physiol* **91**: 1412–1420.

Xu Y (2002). Sphingosylphosphorylcholine and lysophosphatidylcholine: G protein-coupled receptors and receptor-mediated signal transduction. *Biochim Biophys Acta* **1582**: 81–88.

Zhu K, Baudhuin LM, Hong G, Williams FS, Cristina KL, Kabarowski JH *et al*. (2001). Sphingosylphosphorylcholine and lysophosphatidylcholine are ligands for the G protein-coupled receptor GPR4. *J Biol Chem* **276**: 41325–41335.